Formation of Au Nanofiber/Fullerene Nanowhisker 1D/1D Composites via Reductive Deposition at the Interface between an Ionic Liquid and Water

AUTHOR(S):

Koya, Ippei; Yokoyama, Yuko; Sakka, Tetsuo; Nishi, Naoya

CITATION:

Koya, Ippei ...[et al]. Formation of Au Nanofiber/Fullerene Nanowhisker 1D/1D Composites via Reductive Deposition at the Interface between an Ionic Liquid and Water. Chemistry Letters 2022, 51(6): 643-645

ISSUE DATE:

2022-06

URL:

http://hdl.handle.net/2433/275817

Formation of Au nanofiber/fullerene nanowhisker 1D/1D composites via reductive deposition at the interface between an ionic liquid and water

Ippei Koya, Yuko Yokoyama, Tetsuo Sakka, and Naoya Nishi*
Department of Energy and Hydrocarbon Chemistry, Graduate School of Engineering, Kyoto University, Kyoto, 615-8510, Japan

E-mail: nishi.naoya.7e@kyoto-u.ac.jp

Au nanofiber (NF)/fullerene nanowhisker (FNW) 1D/1D composites have been prepared at the liquid/liquid interface between an ionic liquid (IL) and water (W). Au NFs have been reductively deposited on the FNWs adsorbed at the IL/W interface via the electron transfer across the interface between $AuCl_4^-$ in W and a reducing agent in IL, coupled with the ion transfer of $AuCl_4^-$ from W to IL.

Keywords: ionic liquid/water interface | anisotropic Au nanostructures | liquid-liquid interface | ITIES | electrodeposition

Metal nanofibers (NFs), which have unique one-dimensional (1D) nanostructures, exhibit physicochemical properties that are different from those of the bulk metal and even metal nanoparticles. They are expected to be applied in a variety of fields as electronic,[1] optical,[2] electrocatalytic,[3] and catalytic materials.[4,5] The 1D/1D composites of metal NFs combined with non-metallic 1D nanostructures have also been reported, such as those with cellulose NFs,[6-8] aramid NFs,[9] and carbon nanotubes (CNTs),[10] which have both conductivity and flexibility, and are expected to be applied to electromagnetic shielding, transparent conductive films and conductive inks.

The liquid|liquid interface between oil and water has been utilized as a redox reaction site to fabricate metal nanostructures.[11,12] By replacing oil with hydrophobic ionic liquid (IL) in the oil-water two-phase system, we found that metal NFs can be fabricated at the IL|W interface.[13-15] The IL is not just a substitute for oil, rather plays a role as a stabilizer to prevent the aggregation of nanostructures[16] by virtue of the ionic layers spontaneously formed at the growing metal nanostructures.[17-19] The anisotropic growth of metal[20] is likely to be induced by such surface ionic structures as well as the viscosity difference between IL and W.[21]

This methodology to prepare metal NFs at the IL|W interface can be utilized to fabricate their composites with other nanomaterials. For example, by adopting thiophenetrimers as the reducing agent of $AuCl_4^-$ for their redox reaction at the IL|W interface, Au NF/polythiophene (PT) plate composites were fabricated.[22] Au NF/reduced graphene oxide (rGO)[23] and Au NF/CNT[10] composites were prepared by depositing Au NFs on the nanocarbons adsorbed at the IL|W interface. In the present study, we report the fabrication of Au NF/fullerene nanowhisker (FNW) composites, another class of 1D/1D metal/nanocarbon composites, using the IL|W interface method. FNWs are one-dimensional crystals of fullerene molecules bound together by van der Waals forces. One of the characteristics of FNWs is their softness;[24] they can be easily processed into a variety of shapes by bundling. Also, FNWs exhibit superconductivity when doped with potassium.[25] The FNW composites with Au nanoparticles[26-28] have been reported for their catalysis applications. A new methodology to form Au/FNW composites of other types, like Au NF/FNW 1D/1D composites, would be valuable to pursue this direction of application further.

FNWs with a diameter of about 500 nm were prepared following the method previously reported.[29] 4 mL of isopropyl alcohol was added on top of 0.5 mL of a saturated toluene solution of fullerene (nanom purple STL, Frontier Carbon) in a bottle (inner diameter 15 mm) and the liquid-liquid two-phase system was sonicated for 10 seconds. The two-phase system was kept still at 5°C for 24 h during which the two liquids gradually mixed with each other, finally forming one liquid phase with deposited FNWs at the bottom. After removing the supernatant liquid, the FNWs were dried in the bottle in a vacuum box (Sanplatec). The prepared FNWs were observed by scanning electron microscopy (SEM) (Regulus 8220, Hitachi). A SEM image of FNWs is shown in Figure 1. FNWs with a diameter of about 500 nm and a length of about 10 μm were obtained.

A hydrophobic IL, trioctylmethylammonium bis(nonafluorobutanesulfonyl)amide ($TOMAC_4C_4N$), was prepared[30,31] and used as the IL phase. In the IL (0.3 mL) phase, tri-p-tolylamine (TPTA, 100 mmol/kg), a reducing agent, was dissolved. As the W phase, a dispersion of FNWs was prepared by adding 1.6 mL of Mill-Q water to the prepared FNWs in the bottle followed by sonication for 30 s, and it was put on the IL phase. The IL-W two-phase system was kept still for 1 day to adsorb FNWs at the IL|W interface. Then, the dispersion, which was the upper W phase, was replaced with 1.2 mL of HCl solution (0.1 M) containing $AuCl_4^-$ (10 mM), and the IL-W two-phase system was kept still for 1 day to reductively deposite Au on the FNWs at the IL|W interface. The composites on the IL|W interface were dispersed in methanol and transferred to a centrifuge tube. The transferred composites were separated from the liquid by centrifugation at 4000 rpm for 15 min in a centrifuge (CN-1050, AS-ONE) and the supernatant was removed. This washing process was carried out four times with methanol, five times with dichloromethane, and once with methanol. The composites were dried in a vacuum box for 1 day. The structures and compositions of the composites were analyzed by SEM and energy dispersive X-ray analysis (EDX) (Regulus 8220, Hitachi).

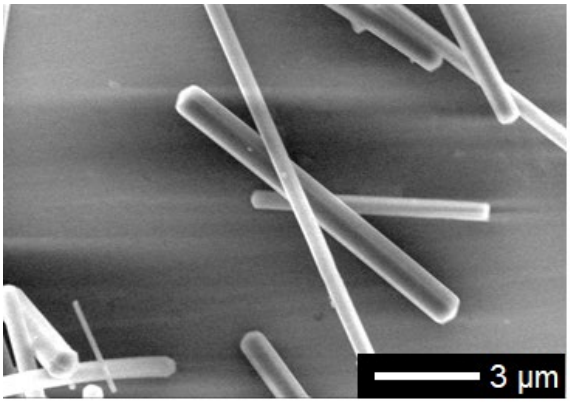

Figure 1. SEM image of FNWs.

The SEM and EDX images of Au NF/FNW composites are shown in Figure 2 and Figure S1, respectively. One can see that Au NFs (50-100 nm diameter[31]) are attached to FNWs (500 nm diameter, see also Figure S1). A control experiment was performed, where fullerene (C60) molecules instead of FNWs were adsorbed on the IL|W interface, and Au was reductively deposited at the IL|W interface (see Supporting Information for details). For this case, composites of Au NFs and C60 aggregates were obtained. These Au NF composites with FNWs and C60 are different from those with PT[21] and CNT,[10] where Janus-type composites were deposited at the IL|W interface, with different Au structures on the W and IL sides. This structural difference can be explained by the reaction mechanism, which will be described below.

To confirm the formation mechanism of Au NF/FNW composites, another control experiment was performed. The deposition of Au NFs occurs only when the ion transfer (IT) of $AuCl_4^-$ from W to IL occurs and then the transferred $AuCl_4^-$ is reduced on the IL side of the interface.[22] To prevent the IT of $AuCl_4^-$ and the subsequent Au NF formation on the IL side of the interface,[22] $C_4C_4N^-$ was added in W (30 mM LiC_4C_4N), which is more hydrophobic than $AuCl_4^-$ and more thermodynamically favored to transfer to IL. As expected in the SEM image (Figure S2), Au NFs disappeared and Au microurchins instead are discernible on the FNWs. The formation of Au microurchins indicates the dendritic growth of Au in a diffusion-limited manner on the W side of the IL|W interface in this $C_4C_4N^-$ added case.[22] In this case, the ET between $AuCl_4^-$ and TPTA starts at the three-phase interface of W, IL, and FNW (see the discussion below and Figure 4a), and the Au nuclei grow toward the W side of the interface because no $AuCl_4^-$ ions are transferred to IL, hampered by the IT of $C_4C_4N^-$. These results indicate that $AuCl_4^-$ ions were transferred to IL and then reduced, forming Au NFs on the IL side of FNWs adsorbed at the IL|W interface.

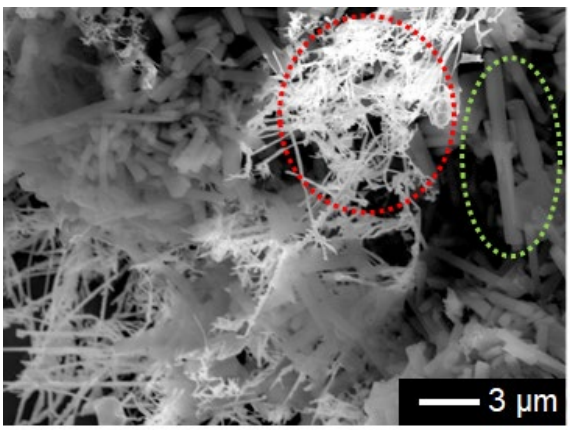

Figure 2. SEM image of Au NF/FNW composites after 24 h reaction. The green and red circles represent FNW and Au NFs, respectively.

Figure 3 shows the time evolution of the structure of the Au NF/FNW composites. 1 h after the start of the reaction, short 1D Au were already attached to the FNWs (Figure 3a). In 5 h, the FNWs were covered with Au NFs (Figure 3b). In other words, the growth of Au NFs started immediately after the start of the reaction. This result is in contrast to the case when Au was deposited on the CNTs adsorbed on the IL|W interface.[10] In the CNT case,[10] Au microurchins were first formed on the W side of the CNTs and then Au NFs appeared 20 h after the start of the reaction.[10]

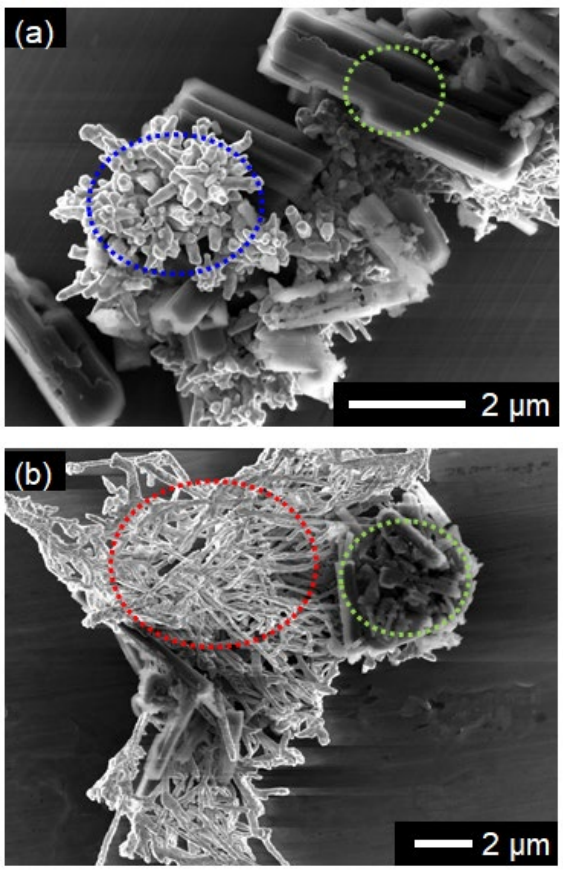

Figure 3. SEM images of Au/FNW composites after (a) 1 and (b) 5 h reaction. The green, blue, and red circles represent FNW, 1D Au, and Au NFs, respectively.

In order to further confirm the orientation of Au NFs, the IL was solidified after the reaction, and the W side of the composites on the surface of the solidified IL was observed by SEM and EDX. This was realized by switching the IL to trioctylmethylammonium tetrakis[3,5-bis(trifluoromethyl)phenyl]borate (TOMATFPB),[22] whose melting point (36 °C) is higher than room temperature. The composites were fabricated at 50 °C. It should be noted that Au NFs are formed at the IL|W interface regardless of the difference in IL kind and reaction temperature (Figure S3). Then the IL-W two-phase system was cooled down to room temperature. The upper W phase was removed and the composites on the solidified IL was analyzed. Au particulates attached to FNWs, rather than Au NFs, were observed (Figure S4), suggesting that Au is reductively deposited at the three-phase interface between W, IL, and FNW, and grows toward the IL side of the IL|W interface.

As described above, the structure of the Au NF/FNW composites was different from the CNT counterpart: Janus-type composites with different Au structures on the IL side (Au NFs) and the W side (Au microurchins) of the CNTs adsorbed at the IL|W interface.[10] This difference can be explained by the conductivity of these nanocarbons; the conductivity of FNWs is significantly low, 10^{-2} S cm^{-1},[32] compared with that of CNTs, 10^{4} S cm^{-1}. It is likely that the CNTs at the IL|W interface can bypass electrons from TPTA on the IL side to $AuCl_4^-$ on the W side, allowing the Au metal formation on the W side, whereas the FNWs cannot, leading to no Au deposit on the W side of the FNWs, and no Au microurchins on the Au NF/FNW composites.

The formation mechanism is proposed as follows (Figure 4). First, Au metal is deposited at the three-phase interface of W, IL, and FNW via the electron transfer between TPTA and $AuCl_4^-$ and IT of $AuCl_4^-$ from W to IL for charge compensation (Figure 4a). Then, the transferred $AuCl_4^-$ is reduced on the IL side, and the anisotropic Au growth is induced with the help of both the ordered interfacial ionic structure and the high viscosity in the IL,[21] leading to the formation of Au NFs (Figure 4b). The IT of liberated Cl^- from IL to W also occurs, which is counterbalanced by further IT of $AuCl_4^-$. As a result, the composites of Au NFs and FNWs were successfully formed at the IL|W interface.

In summary, the reductive deposition of Au on FNWs after adsorption of FNWs onto the IL|W interface resulted in the spontaneous formation of Au NF/FNW composites at the interface. The formation mechanism of the Au NF/FNW composites and their structure were different from those in the case of CNT,[10] another 1D nanocarbon, which is likely due to their conductivity difference.

This work was partly supported by JSPS KAKENHI (no. 21H02046).

Supporting Information is available on http://dx.doi.org/10.1246/cl.******.

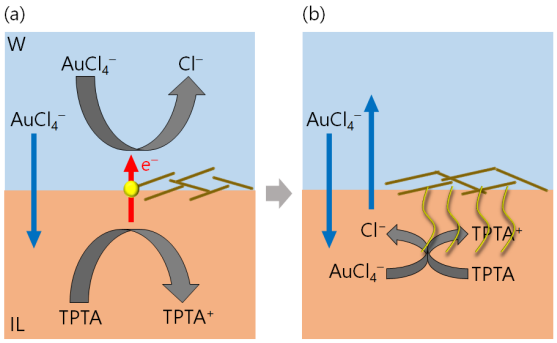

Figure 4. Formation mechanism of Au NF/FNW composites. The blue and red arrows represent the IT and ET across the interface, respectively. The gray arrows are from the reactant to the product of the redox reaction.

References

1 S. Hong, H. Lee, J. Lee, J. Kwon, S. Han, Y.D. Suh, H. Cho, J. Shin, J. Yeo, S.H. Ko, *Adv. Mater.*, **2015**, 34, 744.
2 S. Kundu, *J. Mater. Chem.*, **2013**, 1, 831.
3 S. Du, *Engineering,* **2021**, 7, 33.
4 L.L. Lu, J. Ge, J.N. Yang, S.M. Chen, H. Bin Yao, F. Zhou, S.H. Yu, *Nano Lett.*, **2016**, 16, 4431.
5 H. Xu, H. Shang, C. Wang, Y. Du, *Adv. Funct. Mater.*, **2020**, 30, 1.
6 H. He, R. Chen, L. Zhang, T. Williams, X. Fang, W. Shen, *J. Colloid Interface Sci.*, **2020**, 562, 333.
7 R. Yin, S. Yang, Q. Li, S. Zhang, H. Liu, J. Han, C. Liu, C. Shen, *Sci. Bull.*, **2020**, 65, 899.
8 Y. Chen, S. Yang, Z. Qiu, Y. Li, F. Qiu, T. Zhang, *Cellulose,* **2021**, 28, 8693.
9 S. Li, K. Qian, S. Thaiboonrod, H. Wu, S. Cao, M. Miao, L. Shi, X. Feng, *Compos. Part A Appl. Sci. Manuf.*, **2021**, 151, 106643.
10 I. Koya, T. Sakka, N. Nishi, *Langmuir*, **2021**, 37, 9553.
11 Y. Cheng, D.J. Schiffrin, *J. Electroanal. Chem.*, **1996**, 92, 3865.
12 A. Trojánek, J. Langmaier, Z. Samec, *J. Electroanal. Chem.*, **2007**, 599, 160.
13 Y. Zhang, N. Nishi, K. ichi Amano, T. Sakka, *ACS Appl. Mater. Interfaces.*, **2018**, 282, 886.
14 Y. Zhang, N. Nishi, T. Sakka, *ACS Appl. Mater. Interfaces.*, **2019**, 11, 23731.
15 Y. Zhang, N. Nishi, T. Sakka, *Colloids Surf. A,* **2020,** 597, 124747.
16 T. Torimoto, T. Tsuda, K.I. Okazaki, S. Kuwabata, *Adv. Mater.*, **2010**, 22, 1196.
17 N. Nishi, T. Uruga, H. Tanida, *J. Electroanal. Chem.*, **2015**, 759, 129.
18 N. Nishi, J. Uchiyashiki, Y. Ikeda, S. Katakura, T. Oda, M. Hino, N.L. Yamada, *J. Phys. Chem. C.*, **2019**, 123, 9223.
19 S. Katakura, K.I. Amano, T. Sakka, W. Bu, B. Lin, M.L. Schlossman, N. Nishi, *J. Phys. Chem. B.*, **2020**, 124, 6412.
20 J. Dupont, J.D. Scholten, *Chem. Soc. Rev.*, **2010**, 39, 1780.
21 T. Kakinami, N. Nishi, K.I. Amano, T. Sakka, *Bunseki Kagaku,* **2016**, 65, 157.
22 N. Nishi, I. Yajima, K.I. Amano, T. Sakka, *Langmuir,* **2018**, 34, 2441.
23 Y. Zhang, N. Nishi, I. Koya, T. Sakka, *Chem. Mater.*, **2020**, 32, 6374.
24 Y. Funamori, R. Suzuki, T. Wakahara, T. Ohmura, E. Nakagawa, M. Tachibana, *Carbon,* **2020**, 169, 65.
25 H. Takeya, R. Kato, T. Wakahara, K. Miyazawa, T. Yamaguchi, T. Ozaki, H. Okazaki, Y. Takano, *Mater. Res. Bull.*, **2013**, 48, 343.
26 J.W. Ko, J. Li, W.B. Ko, *Nanomater. Nanotechnol.*, **2015**, 5, 1.
27 J. Yang, H. Lim, H.C. Choi, H.S. Shin, *Chem. Commun.*, **2010**, 46, 2575.

28 J.W. Ko, J. Li, W.B. Ko, *Fuller. Nanotub. Carbon Nanostructures.,* **2017**, 25, 710.
29 T. Wakahara, K. Miyazawa, Y. Nemoto, O. Ito, *Carbon,* **2011**, 49, 4644.
30 N. Nishi, H. Murakami, Y. Yasui, T. Kakiuchi, *Anal. Sci.,* **2008**, 24, 1315.
31 N. Nishi, T. Kakinami, T. Sakka, *Chem. Commun.,* **2015**, 51, 13638.
32 K. Miyazawa, Y. Kuwasaki, K. Hamamoto, S. Nagata, A. Obayashi, M. Kuwabara, *Surf. Interface Anal.,* **2003**, 35, 117.